VII International Conference on Computational Methods for Coupled Problems in Science and Engineering
COUPLED PROBLEMS 2017
M. Papadrakakis, E. Oñate and B. Schrefler (Eds)

A ONE WAY COUPLED THERMO-MECHANICAL MODEL TO DETERMINE RESIDUAL STRESSES AND DEFORMATIONS IN BUTT WELDING OF TWO ASTM A36 STEEL PLATES

ROSENDO FRANCO*, W. GUILLERMO LOAIZA, PAUL P. LEAN AND HERBERT YÉPEZ

Grupo de Investigación Asistida por Computadora (INACOM/Aula PUCP-CIMNE)
Pontificia Universidad Católica del Perú
Av. Universitaria 1801, Lima 32, Peru
e-mail: rofranco@pucp.edu.pe, http://investigacion.pucp.edu.pe/grupos/inacom/

Key words: Thermo-Mechanical Model, Finite Element Method, Welding Simulation, Residual Stresses

Summary: To simulate the gas metal arc welding (GMAW) process in two ASTM A36 steel plates a finite element numerical model was developed, to obtain the corresponding residual stresses and deformations. The welding process was simulated as a one way coupled thermo-structural problem, considering that the structural field has very little influence in the thermal field, which is widely accepted in the specialized literature. To solve the thermal field, a nonlinear transient problem was created using finite second order elements that have temperature as the only degree of freedom in their nodes. The thermal properties of material were defined as a function of temperature and a combined convection-radiation coefficient was used as boundary condition. The double ellipsoidal model presented by Goldak was used to simulate the heat source and its dimensions were determined from the expressions developed by Christensen. To solve the structural field another nonlinear transient problem was created, considering the same mesh and the same time step of the thermal problem, using finite second order elements that have three displacements as degrees of freedom in their nodes. The mechanical properties of material were defined as a function of temperature, a thermo-elasto-plastic material model was used and the necessary displacement constraints were applied as boundary conditions. The temperature distribution obtained by solving the thermal field at each time step was transferred as a load to the structural problem. In both problems the "birth and death" technique was used to simulate the material deposition, which is implemented in the ANSYS software used in the present study. The activation of "dead" elements of the weld bead in the thermal analysis was performed simultaneously with the passage of the heat source, while in the structural analysis "dead" elements were activated as a function of their temperature. Different activation temperatures of "dead" elements were tested in the structural analysis, obtaining the best results when this temperature takes a value of 80% of material solidification temperature. The model used in this study was validated experimentally, taking as reference the residual displacements in several points of the welded plates. It was verified that there is a good correspondence between numerical and experimental results, with an error of less than 10%.

1 INTRODUCTION

The arc welding process encapsulates several coupled physical phenomena: fluid flow in the weld pool, heat flow in the structure, microstructural evolution of the materials, stress development and distortion of the structure. Theses phenomena have to be modeled as multi-physics problem. The mechanical response of welds is sensitive to the close coupling between thermal energy distribution, microstructure evolution and mechanical behavior. Figure 1 describes the coupling between the different fields in the modeling of welding, where the solid arrows denote strong coupling and the dotted arrows denote weak coupling [1].

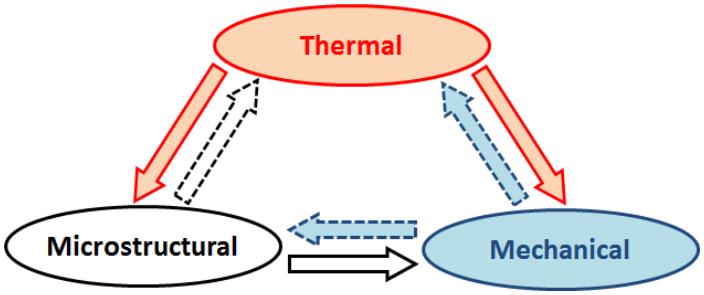

Figure 1: Coupling between different fields in welding analysis [1].

When the purpose of the analysis is to determine residual stresses and deformations of the structure, most authors use the simplest approach, i.e., considers only the one way coupled thermo-mechanical problem. The efforts of investigations are more focused on two main issues: the heat source model used in the thermal problem and the material behavior model used in the mechanical problem. In addition, it is necessary to take into account other important aspects in order to obtain accurate results. Temperature dependent material properties, thermal and mechanical boundary conditions and the material deposition method have significant influence in the simulation results.

In this paper the one way coupled thermo-mechanical approach is used and some important related topics are discussed. Consequently, a finite element numerical model was developed to obtain residual stresses and deformations of welded structure. Finally, the model was applied in the butt welding (GMAW) process of two ASTM A36 steel plates and compared with experimental results.

2 HEAT SOURCE MODEL

It is important to select an appropriate heat source model to obtain the accurate temperature distribution results, which will have a significant impact on the mechanical results, i.e., on the residual stresses and deformations. Especially, the choice of the heat source is sensitive for the results obtained in the fusion zone (FZ) and the heat affected zone (HAZ).

The investigations related to the models of heat sources date from 1935 when Rosenthal started his theoretical studies about arc welding processes. In his works, he has proposed point, linear and plane heat source models [2]. However, measurements of temperatures in the fusion and heat affected zones differ significantly from the values provided by those solutions, since the singularity located at the source origin results in infinite temperature levels [3]. In his book *Thermal Analysis of Welds* Nguyen [4] presents various analytical

solutions for stationary and moving heat sources models, including the Gaussian distributed volumetric heat source. Jeyakumar et al. [5] used this approach to evaluate residual stress in butt welded joint of ASTM A36 steel plates and found good agreement with experimental and others results. Stamenkovic and Vasovic [6] used a simplify method by assuming the welding arc stayed at an element with a constant specific volume heat generation, and then moved to the next element at the end of the load step as the welding was finished.

There is a great variety of models of heat sources documented in the literature but undoubtedly it is the double ellipsoidal model developed by Goldak and Akhlaghi [7] the most used by the researchers in arc welding simulations. Batista et al. [8] used Goldak's model to determine residual stresses in ASTM AH36 steel welded by TIG process. The same model was used by Malik et al. [9] to study circumferentially arc welded thin-walled cylinders to investigate the residual stress fields. The results of simulation in this work show great accuracy for transient temperature distribution and residual stresses in comparison with experimental results they performed. Qureshi et al. [10], Fu et al. [11], Pasternak et al. [12], Wang et al. [13], Chand et al. [14], Nuraini et al. [15], Abit et al. [16], Asserin et al. [17] and many others researchers also used this model in their investigations.

Figure 2 shows the double ellipsoidal model presented by Goldak that has been selected to develop the present work due to its great acceptance.

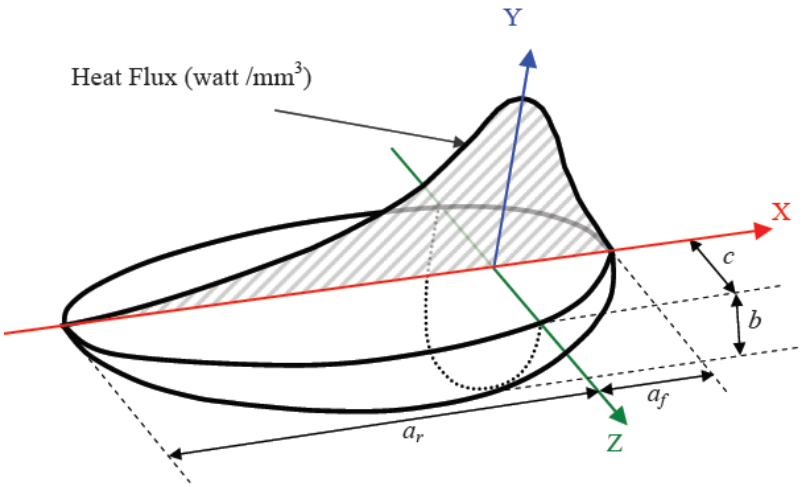

Figure 2: Goldak's double ellipsoidal heat source model [9].

The input heat for the front heat source is:

$$q_f(x,y,z,t) = \frac{6\sqrt{3}\cdot f_f \cdot Q}{\pi\sqrt{\pi}\cdot a_f \cdot b \cdot c} \cdot exp\left(\frac{-3(x-v\cdot t)^2}{a_f^2} + \frac{-3y^2}{b^2} + \frac{-3z^2}{c^2}\right) \quad (1)$$

For the rear heat source is:

$$q_r(x,y,z,t) = \frac{6\sqrt{3}\cdot f_r \cdot Q}{\pi\sqrt{\pi}\cdot a_r \cdot b \cdot c} \cdot exp\left(\frac{-3(x-v\cdot t)^2}{a_r^2} + \frac{-3y^2}{b^2} + \frac{-3z^2}{c^2}\right) \quad (2)$$

Where a_f, a_r, b and c are the ellipsoid dimensions. The parameters f_f and f_r give the

fractions of the heat in the front and rear parts of the source and have to meet the condition $f_f + f_r = 2$. The total heat gained from the welding arc is $Q = \eta \cdot V \cdot I$, η is the efficiency of the arc, V is the welding voltage and I is the welding current. The welding speed is v and t is the time.

The greatest difficulty with the use of the heat source proposed by Goldak is the determination of its geometric and energetic parameters. Some authors recommend to determine the geometric parameters of the ellipsoid (a_f, a_r, b and c) experimentally an calibrate the energetic parameters (f_f and f_r). Batista et al. [8] determined the geometric parameters by metallographic analysis and the energy parameters were obtained with the support of the relationships found in the literature. Asserin et al. [17] adjusted all used parameters by inverse methods from experimental results. To predict the heat source model parameters a neural network was used by Fu et al. [11].

When no experimental data is available, a possible option is to use the procedure developed by Christensen [18]. This procedure proposes empirical expressions and curves based on experimental tests to determine the geometric parameters of the heat source. In order to use the procedure, the parameters of the welding process (Q, v) and some properties of the material are required. Detailed information can be found in [18]. In addition, due to the condition of continuity of the volumetric heat source, the values of q_f and q_r given by equations (1) and (2) must be equal at the $x = 0$ plane. From that condition, another constraint is obtained for energetic parameters as $f_f/a_f = f_r/a_r$. Subsequently, the values for these two coefficients are determined as $f_f = 2 \cdot a_f/(a_f + a_r)$; $f_r = 2 \cdot a_r/(a_f + a_r)$ [19]. The Christensen procedure and the condition of continuity are used in the present paper.

3 MATERIAL BEHAVIOR MODEL

In his paper Lindgren [20] points out that it is important to have a correct description of the material behavior in order to have an accurate model and concludes that the most important mechanical properties are Young's modulus, thermal dilatation, and parameters for the plastic behavior.

The constitutive model of the mechanical analysis can be expressed by the total strain increment $\Delta\varepsilon$ obtained from equation (3) [11,13].

$$\Delta\varepsilon = \Delta\varepsilon^e + \Delta\varepsilon^p + \Delta\varepsilon^T + \Delta\varepsilon^{creep} + \Delta\varepsilon^{tran} \tag{3}$$

Where $\Delta\varepsilon^e$, $\Delta\varepsilon^p$, $\Delta\varepsilon^T$ and $\Delta\varepsilon^{creep}$ are the elastic, plastic, thermal and creep strain increments, respectively. $\Delta\varepsilon^{tran}$ is the strain induced by the phase transformation. Like [11], the phase-transformation related strain increment was neglected in the present work because it has an insignificant contribution to the total strain in low-carbon steel. Considering that welding process is a very short heating process, $\Delta\varepsilon^{creep}$ was also not included in the present study.

Almost all authors that simulate welding processes consider rate-independent plasticity because the material has a high temperature during a relatively short time of the weld thermal cycle, and therefore the accumulated rate-dependent plasticity is neglected [20]. Rate-independent plasticity is characterized by three parameters, they are the yield criterion, the flow rule and the hardening law [20,21].

The model that has been used most widely for rate-independent plasticity is the von Mises

yield criterion given by equation (4), where σ_1, σ_2 and σ_3 are the principal stresses. Malik et al. [9], Qureshi et al. [10], Pasternak et al. [12], Wang et al. [13], Chand et al. [14] and Asserin et al. [17] used von Mises yield criterion in their works. The flow rule states that the plastic flow is orthogonal to the yield surface.

$$\sqrt{\frac{(\sigma_1 - \sigma_2)^2 + (\sigma_2 - \sigma_3)^2 + (\sigma_3 - \sigma_1)^2}{2}} = \sigma_y \tag{4}$$

A hardening law is needed to determine the amount of plastic flow and the evolution of the yield strength of the material [20]. Wang et al. [13] describe and uses four possible hardening laws: (1) perfect plasticity; (2) isotropic hardening; (3) kinematic hardening; (4) combined hardening (isotropic and kinematic). Pasternak et al. [12] used isotropic hardening law. While Malik et al. [9], Qureshi et al. [10], Chand et al. [14] and Asserin et al. [17] used kinematic hardening law.

Taking in to account the literature review a thermo-elasto-plastic material formulation has been chosen for the present research considering the von Mises yield criterion with associated flow rule and the bilinear kinematic hardening model.

4 TEMPERATURE DEPENDENT MATERIAL PROPERTIES

The thermal problem consists in solving the energy conservation equation (5) [10,13,14].

$$\rho c \frac{\partial T}{\partial t}(x, y, z, t) = -\nabla \cdot q(x, y, z, t) + Q(x, y, z, t) \tag{5}$$

Where, ρ is the density of the material, c is specific heat capacity, T is current temperature, q is heat flux vector, Q is internal heat generation rate, t is the time, ∇ represents the spatial gradient operator and x, y, z are the coordinates in the reference plane. The nonlinear isotropic Fourier heat flux constitutive equation is given by (6) [10,14], where k is the temperature dependent thermal conductivity.

$$q = -k \cdot \nabla T \tag{6}$$

As can be seen the thermal properties required to solve the thermal problem are: material density, specific heat and thermal conductivity, all of which are temperature dependent. It would be necessary to know the values of these properties in function of the temperature in order to perform a thorough analysis. Some authors take constant the material density specifically when dealing with steels [9,10].

The mechanical properties required to simulate the mechanical problem are related to the material behavioral model used, which for this study is a thermo-elasto-plastic model with von Mises yield criterion and bilinear kinematic hardening model. Therefore, the modulus of elasticity, the Poisson coefficient, the yield stress, the tangent modulus and the coefficient of thermal expansion are required. All these properties are also temperature dependent.

5 THERMAL AND MECHANICAL BOUNDARY CONDITIONS

The boundary conditions in the thermal problem are referred to the dissipation mechanisms of the heat generated during the welding process, which are the convection and the radiation mechanisms. The current tendency is to use a total temperature dependent heat transfer

coefficient h_{total} to simulate a combined thermal boundary condition, both thermal convection and radiation [10,11,14,17]. Combined heat transfer coefficient can be calculated by equation (7).

$$h_{total} = h + \varepsilon \cdot \sigma \cdot (T + T_{amb}) \cdot (T^2 + T_{amb}^2) \quad (7)$$

Where h is the thermal convection coefficient that is dependent on temperature, ε is the radiation emissivity, σ is Stefan Boltzmann constant (5.67×10^{-8} W m^{-2} K^{-4}), T is the current temperature and T_{amb} is the room temperature. In the present study the combined heat transfer coefficient by (7) is used and applied on all the applicable surfaces including the surface of the weld bead.

The boundary conditions in the mechanical problem were defined following the same approach of [11,13]. The nodal temperatures determined in the thermal analysis were applied as thermal loads in the mechanical analysis. The same finite element meshes associated with the stress element and the thermo-mechanical properties were employed in the mechanical analysis. The mechanical boundary conditions were considered to prevent the rigid body motion of the welded plates.

6 MATERIAL DEPOSITION METHOD

Most authors use the element birth and death technique to simulate the metal deposition on the welding bead [5,6,9,10,15,16,22]. Fanous et al. [23] propose a different method called element movement technique. Other authors do not consider the metal deposition effect or do not refer its consideration [11,13]. Some researchers report difficulties with the birth and death technique. Malik et al. [9] and Qureshi et al. [10] report the possibility of excessive distortion issues in mechanical analysis.

Malik et al. [9], Qureshi et al. [10] and Abit et al. [16] describe the use of the birth and death technique and suggest some recommendations. The whole finite element model is generated in the start. Before first time step all elements representing filler metal are deactivated by assigning them a very low value of conductivity in thermal analysis and very low value of stiffness in mechanical analysis. During the thermal analysis, all the nodes of deactivated elements (except those shared with the base metal) are also fixed at ambient temperature till the birth of the respective element. Deactivated elements are re-activated sequentially when they come under the influence of the heat source. During the mechanical analysis a sequential birth of an element takes place when the element reaches the solidification temperature. In this moment the initial strains in the element are set to zero. Melting and ambient temperatures are set as the temperatures at which thermal strains are zero for thermal expansion coefficients of the filler and base metals. Additional recommendations are reported by Lindgren [24]. For better computational results the heat source is supposed to stay at least once on each element along the welding line, so that the heat input algorithm does not miss elements passed during a time step increment.

The model developed in the present study implements the element birth and death technique and collects all previous recommendations. However, in the present work the effect of the activation temperature of death element is evaluated in the mechanical analysis, including the solidification temperature and lower values. The reason for doing so is due to the researchers' interest in exploring an alternative to calibrate the FE model and perhaps to mitigate the excessive distortion reported by other authors.

7 METHODOLOGY

Considering the information collected and discussed in the previous sections, the flowchart shown in figure 3 was elaborated, establishing the general methodology used in the present investigation.

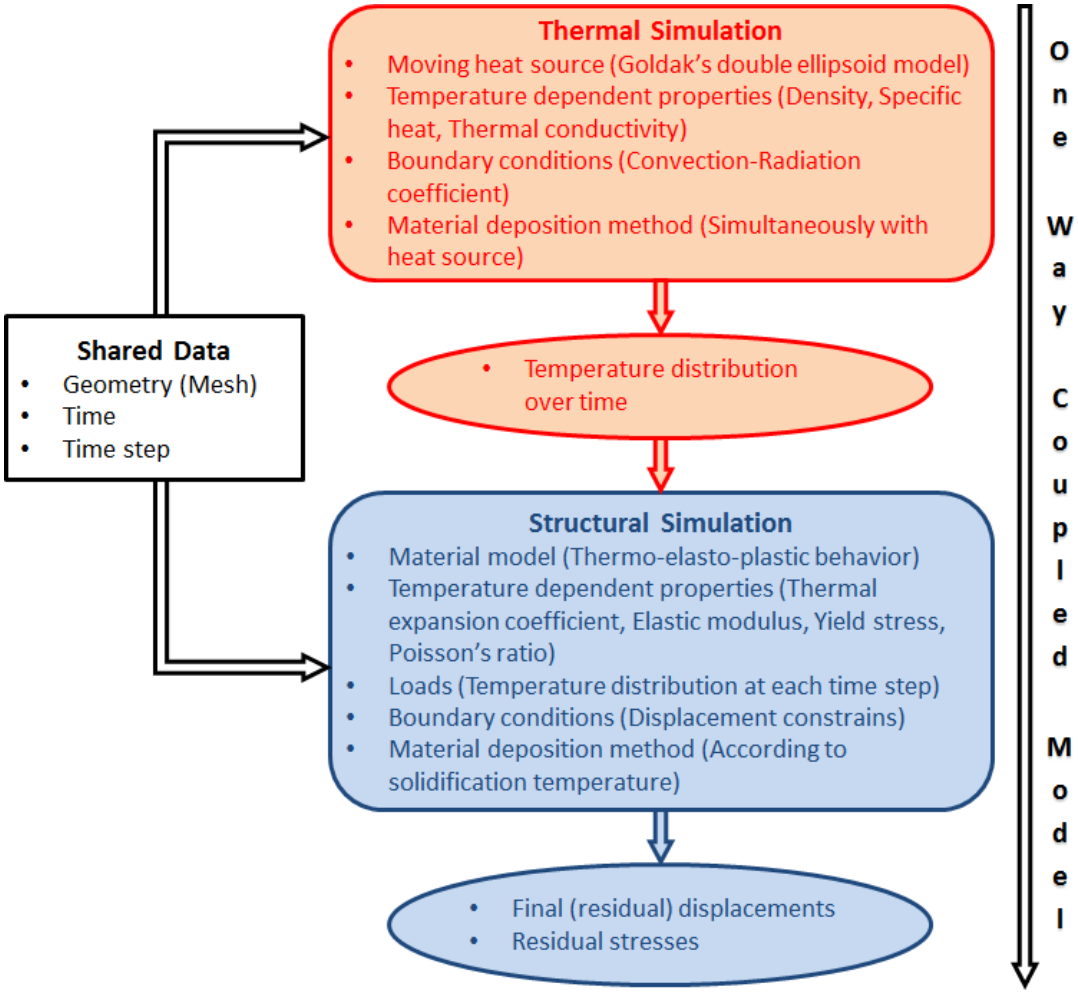

Figure 3: Flowchart of one way coupled model for analysis of residual stresses and deformations.

8 CASE STUDY: BUTT WELDING OF TWO ASTM A36 STEEL PLATES

The finite element numerical model described in the previous sections was used to simulate the gas metal arc welding (GMAW) process in two ASTM A36 steel plates. The objective is to determine the residual stresses and deformations of the welded plates and validate the model with experimental data obtained by the authors. The temperature dependent material properties considered in this study are shown in table 1 [5]. The parameters of the welding process are the same for the numerical analysis as for the experimental tests and are shown in table 2. The Golda's heat source parameters were estimated by using the Christensen procedure and the condition of continuity explained in section 2. The values are shown in table 3.

Table 1: Temperature dependent material properties [5].

Temp (K)	Density (kg/m^3)	Thermal conductivity W/(m·K)	Specific heat (J/(kg·K))	Elastic modulus (GPa)	Poisson's ratio	Thermal expansion coefficient (K^{-1})·10^{-5}	Yield stress (MPa)
298	7880	60	480	210	0.3	1.15	380
373	7880	50	500	200	0.3	1.2	340
473	7800	45	520	200	0.3	1.3	315
673	7760	38	650	170	0.3	1.42	230
873	7600	30	750	80	0.3	1.45	110
1073	7520	25	1000	35	0.3	1.45	30
1273	7390	26	1200	20	0.3	1.45	25
1473	7300	28	1400	15	0.3	1.45	20
1673	7250	37	1600	10	0.3	1.45	18
1773	7180	37	1700	10	0.3	1.45	15

Table 2: Welding process parameters.

Voltage (V)	Current (A)	Velocity (mm/s)	Efficiency (%)
21.1	133	9.5	80

Table 3: Golda's heat source parameters.

Parameter	Value
Length of front ellipsoidal, a_f (mm)	2.02
Length of rear ellipsoidal, a_r (mm)	6.41
Depth of heat source, b (mm)	2.13
Half width of heat source, c (mm)	1.92
Fraction of heat in front ellipsoidal, f_f	0.48
Fraction of heat in rear ellipsoidal, f_r	1.52

8.1 Geometric model and mesh

The geometric model of the welded plates with dimensions is shown in figure 4 a) and consists of a welding coupon 140 mm wide, 3 mm thick and 300 mm long. The discretization of the geometric model was performed with the second order brick elements available in the ANSYS software library used in this work. For the thermal analysis the SOLID279 element was used and for the mechanical analysis the SOLID186 element was used. This way the same mesh can be used for the thermal and mechanical analyzes. Based on maximum reached temperature a mesh sensitivity analysis was performed [9,11]. The final mesh of the model with 132460 elements was chosen for the analysis in order to ensure the mesh independent results. Such a mesh is shown in figure 4 b) with a detail of the weld bead zone.

8.2 Boundary conditions

The combined heat transfer coefficient determined by equation (7) was applied as the thermal boundary condition on all the applicable surfaces including the surface of the weld bead. The emissivity $\varepsilon = 0.51$ and $T_{amb} = 300$ K were considered for the simulation. The temperature dependent thermal convection coefficient h was adopted according to [10].

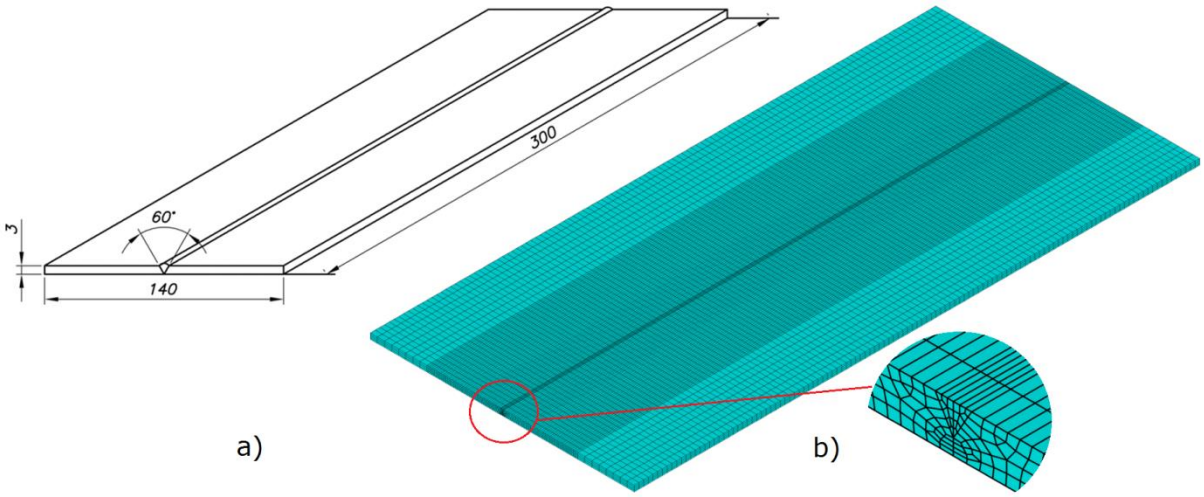

Figure 4: Geometric model. a) Dimensions. b) Mesh and a detail of the weld bead zone.

The nodal temperatures determined in the thermal analysis were applied as thermal loads in the mechanical analysis each time step. The mechanical boundary conditions were considered to prevent the rigid body motion of the welded plates, i.e., normal displacement constrain of the symmetry plane, displacement constrain of two extreme points in vertical (y) direction and displacement constrain of one extreme point in longitudinal (z) direction. The mechanical boundary conditions are shown in the figure 5.

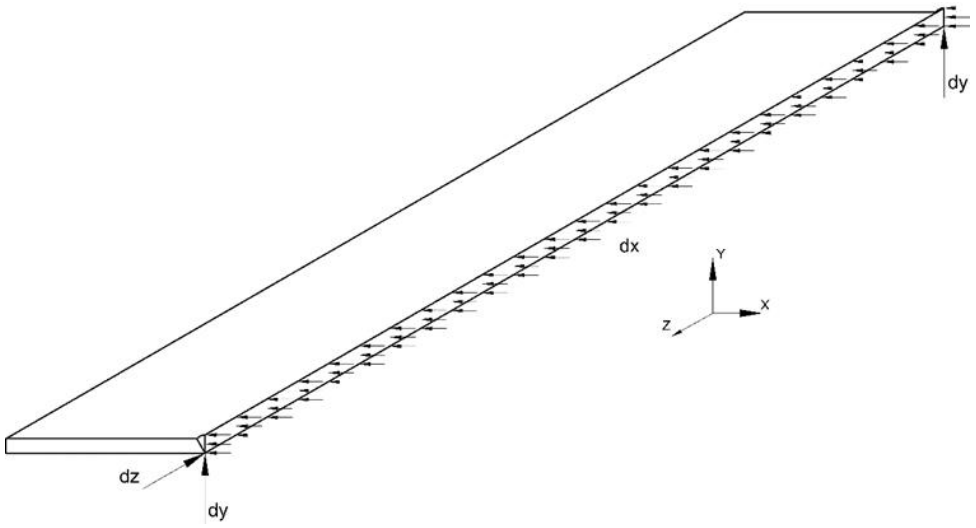

Figure 5: Mechanical boundary conditions.

8.3 Simulation strategy

The methodology described above was implemented in the ANSYS Mechanical APDL environment through macros developed by the authors.

Transient, non–linear thermal and mechanical problems were defined using temperature dependent properties. The welding time was determined considering the welding process

parameters obtaining 31.58 s. An additional time of 2000 s was estimated for the cooling phase. During analyzes the full Newton-Raphson iterative method with a direct sparse matrix solver was used for obtaining the solutions according to [9,10] recommendations..

8.4 Simulation results

Figure 6 a) shows the temperature distribution at the end of the welding time (31.58 s). Figure 6 b) illustrates the temperature profile of five different points up to a time of 100 s. Point 1 is located on the welding line and reaches the highest temperature peak (2240 K).

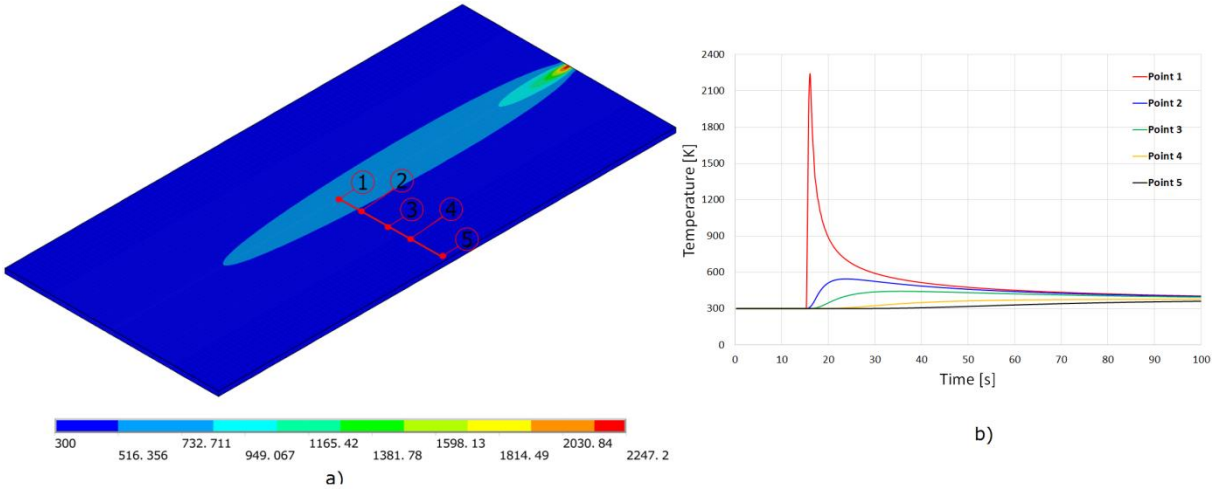

Figure 6: Thermal results. a) Temperature distribution. b) Temperature profile at five different locations.

Figure 7 a) shows that the transverse residual stresses reach a maximum value of 557 MPa. Residual deformations are shown in figure 7 (b). The maximum displacement is reached at the midpoint of the outer edge of the welded plate with a value of 2.76 mm. Simulations of the mechanical problem were performed for three different activation temperatures of death elements (60%, 80% and 100% of material solidification temperature). The results shown in figure 7 correspond to an activation temperature of 80% of the solidification temperature. This setting gives more accurate results.

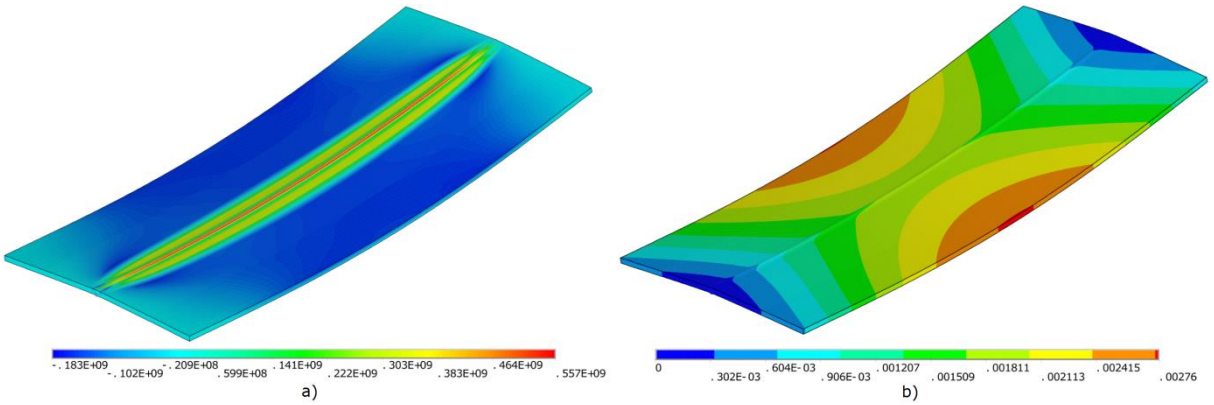

Figure 7: Mechanical results. a) Residual stresses in transversal direction. b) Residual displacements.

8.5 Experimental tests

To validate the developed model, the authors performed experimental tests with the help of a semiautomatic welding machine with GMAW technology. In figure 8 a) the coupons can be seen and in figure 8 b) the arrangement before starting the welding.

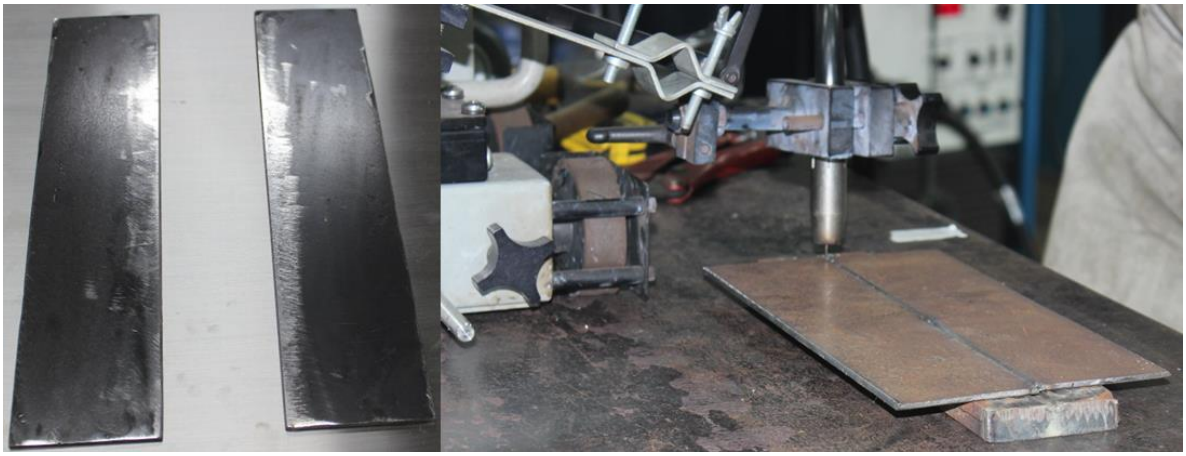

Figure 8: Mechanical results. a) Residual stresses in transversal direction. b) Residual displacements.

After welding and cooling the welded plates, residual displacements at the edges of the plates were measured and an average displacement was obtained. In figure 9 the average experimental result is compared with the numerical results corresponding to the three evaluated activation temperatures. It may be noted that the result for an activation temperature of 60% of the solidification temperature is significantly away from the experimental results. Even though at first glance the results for 80% and 100% appear very similar and better match the experimental result, the results for 80% show a lower standard deviation. In this case the maximum absolute error is about 9.6%.

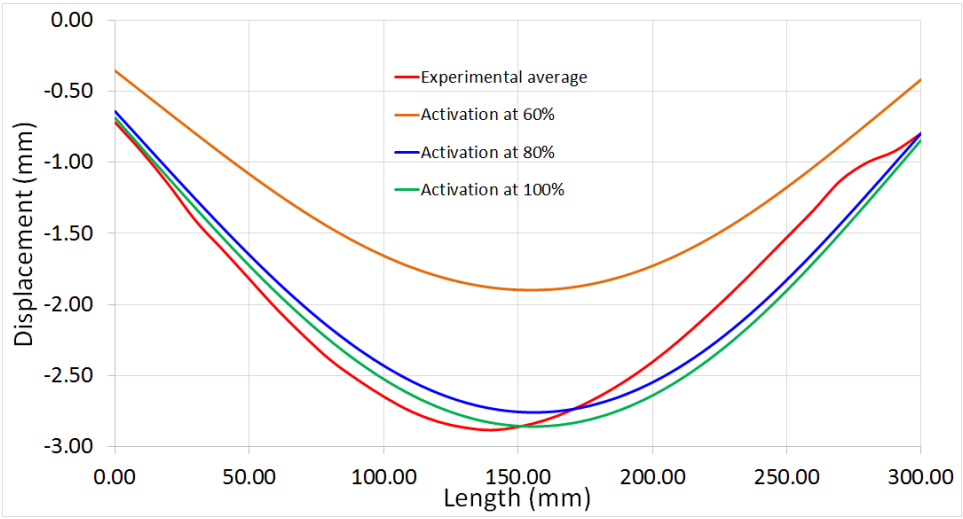

Figure 9: Comparison between numerical and experimental results.

9 CONCLUSIONS

- Based on the best practices reported in the specialized literature, a one way coupled thermo-mechanical model to determine residual stresses and deformations in butt welding of two ASTM A36 steel plates was developed. The model used in this study was validated experimentally by means of measurement of residual displacements in several points of the welded plates. The displacements along the both external sides of the welded plates was averaged and plotted together with numerical results. It was verified that there is a good agreement between numerical and experimental results, with an absolute error of less than 10%.
- Three different activation temperatures of "dead" elements were tested in the structural analysis (60%, 80% and 100% of material solidification temperature). The minimum standard deviation and minimum absolute error were obtained when this temperature takes a value of 80% of material solidification temperature. The evaluation of a greater number of activation temperatures is necessary to reach more conclusive results. It would also be important to analyze the molten zone (FZ) and to evaluate the local behavior when these activation temperatures below the solidification temperature are used.

REFERENCES

[1] Sen, D. *Coupled Field Modeling of Gas Tungsten Arc Welding*. Dissertation for the degree of Doctor of Philosophy in Mechanical Engineering, Virginia Polytechnic Institute and State University, 2012.

[2] Rosenthal, D. Mathematical theory of heat distribution during welding and cutting. *Welding Journal*, vol. 20, n. 5, pp. 220-234, 1941.

[3] Fassani, R.N.S. and Trevisan, O.V. Analytical modeling of multipass welding process with distributed heat source. *Journal of Brazilian Society of Mechanical Sciences and Engineering*, Vol.25, No.3, pp.302-305, 2003.

[4] Nguyen, N.T. *Thermal Analysis of Welds*. WIT Press, Southampton, UK, 2004.

[5] Jeyakumar, M., Christopher, T. and Nageswara Rao, B. Residual Stress Evaluation in Butt Welded Joint of ASTM A36 Steel Plates. *International Journal of Electronics Communication and Computer Engineering*, Vol. 4 (2), pp. 581-587, 2013.

[6] Stamenkovic, D. and Vasovic, I. Finite Element Analysis of Residual Stress in Butt Welding Two Similar Plates. *Scientific Technical Review*, Vol. LIX (1), pp. 57-60, 2009.

[7] Goldak, J. A. and Akhlaghi, M. *Computational Welding Mechanics*. Springer Science+Business Media, Inc., 2005.

[8] Batista, P., Almeida, P., Prasad, Y., Andrade, J., Veras, A., and Sanguinetti, R. Determination of Residual Stresses Numerically Obtained in ASTM AH36 Steel Welded by TIG Process. *Materials Sciences and Applications*, Vol. 4, pp. 268-274, 2013.

[9] Malik, A. M., Qureshi, E. M., Dar, N. U. and Khan, I. Analysis of circumferentially arc welded thin-walled cylinders to investigate the residual stress fields. *Thin-Walled Structures*, ELSEVIER, 2008.

[10] Qureshi, E. M., Malik, A. M. and Dar, N. U. Residual Stress Fields due to Varying Tack Welds Orientation in Circumferentially Welded Thin-Walled Cylinders. *Advances in Mechanical Engineering*, 2009.

[11] Fu, G., Lourenço, M. I., Duan, M. and Estefen, S. F. Influence of the welding sequence on residual stress and distortion of fillet welded structures. *Marine Structures*, ELSEVIER, 2015.
[12] Pasternak, H., Launert, B. and Krausche, T. Welding of girders with thick plates-fabrication, measurement and simulation. *Journal of Constructional Steel Research*, ELSEVIER, 2015.
[13] Wang, Q., Liu, X.S., Wang, P., Xiong, X. and Fang, H.Y. Numerical simulation of residual stress in 10Ni5CrMoV steel weldments. *Journal of Materials Processing Technology*, ELSEVIER, 2016.
[14] Chand, R. R., Kim, I. S., Wu, Q. Q., Kang, B. and Shim, J. Prediction of residual stress and welding deformation in butt-weld joint for different clamped position on the plates. *Int. Journal of Eng. Science and Innovative Tech.* (IJESIT), Volume 3, Issue 5, 2014.
[15] Nuraini, A. A., Zainal, A. S. M. and Azmah Hanim, M.A. The effect of welding process parameter on temperature and residual stress in butt-joint weld of robotic gas metal arc welding. *Australian Journal of Basic and Applied Sciences*, 7(7), pp. 814-820, 2013.
[16] Abid, M., Siddique, M. and Mufti, R. A. Prediction of welding distortions and residual stresses in a pipe–flange joint using the finite element technique. *Modelling Simul. Mater. Sci. Eng.* 13, pp. 455-470, 2005.
[17] Asserin, O., Loredo, A., Petelet, M. and Iooss, B. Global sensitivity analysis in welding simulations - What are the material data you really need? *Finite Elements in Analysis and Design*, 47, pp. 1004-1016, 2011.
[18] Christensen, N., Davies, V. and Gjermundsen, K. Distribution of temperatures in arc welding. *British Welding Journal*, 12(2), pp. 54-75, 1965.
[19] Nguyen, N. T., Ohta, A. and Matsuoka, K. Analytical solutions for transient temperature of semi-infinite body subjected to 3-D moving heat sources. *Welding Journal*, Vol. 78 Issue 8, pp. 265-274, 1999.
[20] Lindgren, L. E. Finite element modeling and simulation of welding. Part 2: Improved material modeling. *Journal of Thermal Stresses*, 24, pp. 195-231, 2001.
[21] Manitaras, T. I. *Elastoplastic Constitutive Models in Finite Element Analysis*. Master Thesis, National Technical University Athens, School of Civil Engineering, Institute of Structural Analysis & Seismic Research, 2012.
[22] Pavani, P., Sivasankar, P., Lokanadham, P. and Uma Mhahesh, P. Finite Element Analysis of Residual Stress in Butt Welding of Two Similar Plates. *International Research Journal of Engineering and Technology*, Vol. 7 (7), pp. 479-486, 2015.
[23] Fanous, I. F. Z., Younan, M. Y. A. and Wifi, A. S. 3-D finite element modeling of the welding process using element birth and element movement techniques. *Journal of Pressure Vessel Technology*, Vol. 125 Issue 2, pp. 144-150, 2003.
[24] Lindgren, L. E. Computational weld mechanics: thermo-mechanical and microstructural simulations. *Woodhead Publishing*, 2007.